29. This conclusion is not changed by a consideration of propagation effects in the interstellar medium over distances of $\lesssim 100$ light years. These include free-free absorption, frequency dispersion, Faraday rotation, scintillations, and other multipath effects.
30. The minimum level of flux density for this distance (from Eq. 3), $S_{min} = 7.1 \times 10^{-27}$ watt m^{-2} hertz^{-1} = 0.71 jansky, at first sight seems far below modern standards in radio astronomy, but it must be remembered that the signal is wholly contained within the very narrow bandwidth of 0.1 hertz. Using such a bandwidth also obviates any concern that normal radio emission from the sun might be detrimental, since its flux density in the UHF range would be ~ 1000 times weaker. The calculated range is somewhat smaller than that derived in the Project Cyclops study (*4*, p. 59), but our value is more realistic.
31. The figure $\sim 2 \times 10^4$ is derived from (i) the required 5-Mhz bandwidth, which yields receiver noise $(5 \times 10^6/0.1)^{1/2}$ worse than that for the carrier alone; (ii) the total signal with the broad bandwidth improving by only a factor of ~ 2; and (iii) "decent picture" implying a dynamic range of ~ 5 in black-to-white AM voltage level. Furthermore, in addition to the need to test myriad possibilities for the various electronic conventions (although the line synchronization rate of ~ 16 khz and the picture rate of ~ 30 hertz would be immediately apparent from a spectral analysis of the signal), the observer of our culture must also compensate for frequency dispersion across the bandwidth arising as the signals traverse the interstellar plasma. For UHF frequencies of ~ 500 Mhz, this amounts to ~ 3 μsec per 5 Mhz for each light year of distance (assuming an electron density of 0.03 cm^{-3}). Once the correct dispersion factor was found, this could be used as a rough indicator of the distance to the earth.
32. Ecliptic latitude refers to the angle which a given direction makes with respect to the plane of the earth's orbit about the sun.
33. If the observer should think that for some unknown reason all of the stations were modulating their transmitter frequencies with an annual periodicity, thereby mimicking a Doppler motion, he would even have a possible way to check this. Accurate measurements would reveal that the sidereal-daily period of 23 hours 56 minutes in fact also showed an annual Doppler modulation of ± 1 part in 10^4 (± 10 seconds) over a year. This could reasonably arise only if the planet as a whole were in motion. Measuring daily periods to the required precision should be possible, despite the fact that 10 seconds of time corresponds to an angle of only ~ 2 arc minutes (requiring various parameters, such as antenna patterns and refraction, to be constant to that degree over a year), since the mean period can in principle be deduced from timings of hundreds of stations each day.
34. Changes in the amount and nature of this phase jitter over many annual cycles might even lead an observer to the conclusion that there was an 11-year periodicity (which we call the solar activity cycle) in his data. If he also studied the solar radio continuum over those 11 years, the same periodicity would be found, once again implying a strong solar influence on the earth. Furthermore, the D-layer of the ionosphere strongly absorbs low-band VHF, peaking at local noon (~ 50 percent absorption at $e = 0°$) and at solar maximum. Monitoring of the peak daily intensity of a particular low-band VHF station would then also show an 11-year cycle as well as an annual modulation due to this solar-daily modulation. Thus in the season when he sees many fewer stations (when star-rise occurs in the early morning), the low-band VHF stations that continue broadcasting will in fact be much more intense than average.
35. *National Association of Broadcasters Engineering Handbook* (McGraw-Hill, New York, ed. 6, 1975), chap. 14.
36. Correct assignment of the Doppler-shifted spectral features arising from a particular station at its two daily appearances would be difficult in crowded regions of the spectrum. The observer would find it least confusing to work at first with (i) stations isolated in frequency, time, or both; (ii) stations appearing only once each day; and (iii) stations whose carrier signals can be recognized by other means, such as a distinctive antenna pattern or transmitter instabilities leading to a distinctive short-term behavior of the carrier frequency.
37. The procedure is not unlike the radar astronomer's technique of mapping a planet's surface through the behavior of the returned signal in time delay and Doppler shift, except that the features in the present case are mapped in the $(\Delta t, V_s)$ plane. If the observer were near $\delta \simeq 0°$, however, he could not construct a unique station map since only the absolute value of the latitude of each station is determinable. Furthermore, monitoring the sidereal-daily period over decades might reveal that there were changes in the time lapse Δt between appearances and disappearances of particular stations, the amount of change depending on their latitude. Assuming that this effect was not due to variable station positions on the rotating body, the necessary conclusion would be that the observer's declination is changing. This information, coupled with the observed nonalignment of the earth's orbital and rotational angular momenta ($|\beta| \neq |\delta|$), would naturally lead to an explanation of the motion in terms of a precessional wobble of the planetary axis. Although the presence of the moon cannot be unambiguously deduced from this precession, both the lunar mass and the earth-moon distance can be found from a study of a monthly periodicity in the Doppler shifts of each station. This arises since the earth-moon system can also be considered as a single-lined spectroscopic binary system where the eavesdropper observes the more massive member. The Doppler shift of the earth is only ~ ± 0.01 cos $|\beta|$ km/sec or ~ 4×10^{-8} c, but continuous monitoring of several hundred stations should nevertheless bring this out. The radial velocity curve then yields both the mass of the moon and the earth-moon separation, when it is assumed that (i) the lunar orbit is in the same plane (already determined) as the earth's orbit about the sun, and (ii) the mass of the earth is estimated from its size and an assumed density.
38. For such a case one has 420 kw directed into a beam ~ 2 arc minutes in size (antenna gain of ~ 4×10^7) and a CW phase-encoded radar over a bandwidth as small as a few hertz. The range of detection is ~ 1000 times greater than that for a UHF television station.
39. F. D. Drake, *Technol. Rev.* **78** (No. 7), 22 (1976).
40. *World Radio/Television Handbook* (Billboard, New York, ed. 29, 1975).
41. We are indebted to the many people who have supplied us with detailed information concerning the radio spectrum of our civilization. In particular we thank B. Lloyd of RCA, G. C. Platts of the British Broadcasting Corporation, J. W. Reinold of the Netherlands Post, Telephone and Telegraph Service, R. Mifflin and W. Jamison of KOMO-TV, R. Oldham of KCTS-TV, R. Wills of Pacific Northwest Bell, W. Gamble of the Office of Telecommunications (Department of Commerce), and R. A. Tell of the Environmental Protection Agency. Observations concerning the frequency stability of video carrier signals were obtained for us by E. K. Conklin and J. C. Carter. The production of this article has been assisted by M. Chinn, D. Healy, and D. Azose, and the contents have greatly profited from criticisms and suggestions by P. E. Boynton, F. D. Drake, R. A. Sramek, and S. von Hoerner.

Predicting Future Atmospheric Carbon Dioxide Levels

The predictions provide a basis for evaluating the possible impact of the continuing use of fossil fuel.

U. Siegenthaler and H. Oeschger

Since the beginning of industrialization man has been significantly changing the atmospheric carbon dioxide concentration. Until 1974 the fossil fuel CO_2 input into the atmosphere amounted to roughly 21 percent of the preindustrial atmospheric CO_2 content, and as a result the atmospheric CO_2 level increased by about 13 percent. If we continue to exhaust oil and coal reserves at a faster and faster rate, in a few decades the increase of the atmospheric CO_2 concentration will be of the same order of magnitude as the preindustrial CO_2 concentration itself. There is serious concern about the possible environmental consequences of such an increase. The average surface temperature of the earth is about 35°K higher than its radiation temperature of 253°K as seen from interplanetary space (*1*). This is partly due to the so-called greenhouse effect, caused by atmospheric water vapor and CO_2. With a higher CO_2 concentration the greenhouse effect will be enhanced. Using a three-dimensional general circulation model, Manabe and Wetherald (*2*) found that the mean surface temperature would be 2° to 3°K higher for a doubled CO_2 level, with a strong amplification (8° to 10°K warming) in the polar areas. Although some important phenomena, such as changes in cloudiness, could not yet be considered, the climatic models developed so far clearly indicate that man-made CO_2 could trigger climatic changes with seri-

U. Siegenthaler is a research associate and H. Oeschger is a professor of physics at the Physics Institute of the University of Bern, 3012 Bern, Switzerland.

0036-8075-/78/0127-0388$02.00/0

ous consequences for human society. A review of models of the climatic effect has been given by Schneider (*3*).

The CO_2 problem has three aspects (*4*): (i) the prediction of future CO_2 levels, (ii) the climatic consequences of a CO_2 increase, and (iii) the impact a given climatic change will have on man. We intend to discuss here the first aspect only, by means of models for the global CO_2 cycle. Many authors have estimated future CO_2 levels [for example, see (*5–12*)]. Our aim is to compare predictions for various input functions and different model approaches to find the extent to which predictions are possible today and the uncertainties that are involved because of our limited knowledge of the global carbon system. We will not consider basically new models, but instead will restrict ourselves to models for the CO_2 cycle already discussed in the literature.

Summary. Results from different models for the natural carbon dioxide cycle are compared. Special emphasis is given to the type of ocean modeling (diffusive deep-sea or two-box ocean), behavior of the biosphere, and value of the oceanic buffer factor against carbon dixoide uptake. According to the most probable models, the fraction of the cumulative production remaining airborne will be between 46 and 80 percent 100 years from now for any realistic assumptions concerning future carbon dioxide production. For a prescribed maximum increase of 50 percent above the preindustrial carbon dioxide level, the production could grow by about 50 percent until the beginning of the next century, but should then decrease rapidly.

Model Concepts

On time scales of centuries, atmospheric CO_2 exchanges mainly with the carbon in the ocean and in the biosphere (*13, 14*). The CO_2 fluxes out of or into the atmosphere-ocean-biosphere system, such as those due to weathering, sedimentation, or volcanic emissions, are negligible for our purposes, as they total only about 5×10^{-6} of the entire oceanic carbon mass per year (*15*).

For the simulation of systems, it is common to use "well-mixed boxes" (or "compartments"). It is a good approximation to consider a reservoir as a well-mixed box if its internal mixing time is short compared to the time scales of the phenomena discussed, such as exchange with other reservoirs, radioactive decay, or production of matter within the reservoir. In our case, the characteristic times of interest are of the order of a decade to centuries. Therefore, we may represent the atmosphere as a well-mixed box, as its mixing time is a few years.

The ocean, the largest of the three exchanging carbon reservoirs, has a turnover time of the order of 1000 years as determined by means of ^{14}C measurements (*16*). Several CO_2 prognoses have been made on the basis of models in which the ocean consists of two well-mixed boxes (2B models)—namely, a mixed layer or surface ocean, and a "deep sea," which means the whole ocean below the mixed layer (*8–12*). In reality, however, the transition between the mixed layer and the deep sea is continuous, and in view of the long turnover time and the above criterion, the deep sea should not be represented by one well-mixed box. It is therefore not surprising that models with a two-box ocean either fail to give a consistent description of the CO_2 cycle (for instance, giving a wrong natural oceanic ^{14}C distribution when they are fitted to give the correct CO_2 increase) or need additional adjustments to provide satisfactory results. Thus, the mixed layer must be chosen a few hundred meters thick in order to obtain satisfactory results (*8, 10, 17*), while observations yield an average value of about 75 m.

A way to consider the continuous character of oceanic mixing is to describe it by eddy diffusion (*18*), which means that the flux of matter (F) is assumed to be proportional to its concentration gradient ($\partial C/\partial z$)

$$F = -K \frac{\partial C}{\partial z}$$

Broecker *et al.* (*6*) introduced the concept of an eddy-diffusive ocean for estimating future CO_2 levels, but computed the oceanic CO_2 transport only in an approximate way. We present here predictions obtained by means of the box-diffusion (BD) model developed by Oeschger *et al.* (*19*), in which the ocean consists of a mixed-layer box and an eddy-diffusive deep sea below it with a constant eddy diffusivity K; horizontal homogeneity is assumed. All vertical transport processes, including turbulent mixing, formation of deep water in polar seas, and particulate transport of carbon, are thus summarized by eddy diffusion and described by one model parameter, K. The BD model consistently reproduces, besides the observed CO_2 increase, phenomena with very different characteristic time scales—namely, the preindustrial vertical ^{14}C distribution in the ocean, the ^{14}C dilution due to the fossil CO_2 (Suess effect), and finally the ^{14}C increase in the ocean surface after the bomb tests (*19, 20*). Therefore, we can expect that the BD model is suited for reliable forecasts, irrespective of the time constants of future variations in CO_2 production. For comparison, we also present results of a 2B model. Figure 1 shows the BD model schematically.

Carbon dioxide exchange between the atmosphere and the mixed layer is formulated as an exchange between two boxes in the usual way. The exchange coefficient between the atmosphere and the mixed layer and the oceanic transport coefficients—eddy diffusivity in the BD model and the exchange coefficient between the mixed layer and the deep sea in the 2B model—are determined from the preindustrial ^{14}C distribution (95 percent of the atmospheric value for the mixed layer and 84 percent for the total ocean). The gas exchange rate between the atmosphere and the ocean has also been determined by measuring the radon-222 deficiency (difference between the radon-222 concentration and the concentration that would be in equilibrium with its parent isotope, radium-226) in surface waters (*21*), and the results are consistent with the exchange coefficient determined from ^{14}C data. In the 2B model the mixed-layer depth is a free parameter, adjusted so as to predict the observed CO_2 increase, whereas in the BD model the mixed-layer depth is 75 m, independently fixed from oceanographic data.

If the atmospheric CO_2 concentration varies, the amount of dissolved CO_2 gas in the ocean surface layer varies proportionally at chemical equilibrium. Carbon dioxide gas, however, accounts for less than 1 percent of the total inorganic carbon (or "total CO_2") in surface seawater, the main species being bicarbonate (HCO_3^-) and carbonate (CO_3^{2-}) ions. An increase in the CO_2 concentration brings about a shift in the chemical equilibria between dissolved CO_2, HCO_3^-, and CO_3^{2-} such that the relative increase of the total CO_2 concentration is less than that of CO_2 gas alone. This is taken into account by introducing a buffer factor ξ: if the CO_2 pressure is increased by p percent, the total CO_2 concentration of seawater, including dissolved CO_2, HCO_3^-, and CO_3^{2-}, increas-

es by only p/ξ percent (*5, 6, 10*). The factor ξ increases with CO_2 pressure. We will use the following relationship, which we deduced from figure 3 of (*10*)

$$\xi = 9 + 4.9\, p_m/P_m - 0.1\, (p_m/P_m)^2 \quad (1)$$

where p_m is the excess CO_2 pressure in the mixed layer over the preindustrial pressure P_m, and p_m/P_m is therefore the relative increase. The size of the buffer factor determines in a crucial way the ocean's capacity for taking up additional CO_2. Different authors who computed ξ from chemical data (equilibrium constants and average seawater composition) obtained, for present CO_2 concentrations, values between 9 and 10, but experiments by Rebello and Wagener (*22*) yielded a value of only 7.

The biosphere, comprising in our case living and dead terrestrial organic matter, is the carbon reservoir about which the least information is available. There is not even agreement on its size; the value given by Bolin (*14*), 1.15×10^{18} grams of carbon, is often quoted, but another estimate leads to nearly 10×10^{18} g (*23*). We take 1.5×10^{18} g, including only long-lived plants (*17*). The biosphere is modeled as a well-mixed box exchanging with the atmosphere. [In the original version of the BD model (*19*) we assumed that all plants have the same lifetime, but an exponential distribution of lifetimes, as given by a well-mixed box, seems more appropriate.]

Some plants probably react to a higher CO_2 level by enhanced photosynthetic activity (*24*), so the biosphere might act as a sink for additional CO_2. This is taken into account in the model in the following way: if the atmospheric CO_2 pressure increases by p percent, the CO_2 flux from the atmosphere to the biosphere increases by ϵp percent. The size of the biosphere growth factor ϵ is uncertain, and values between 0 and 0.3 have been used. On the other hand, it has been suggested that there might be a net decrease of the size of the biosphere due to human influence, resulting in a net flux of biospheric CO_2 into the atmosphere (*4, 25, 26*). If this flux were proportional to the global energy production, it could be formally represented by a negative ϵ. Fertilization by CO_2 and deforestation partly compensate each other, and it is not yet known which effect is prevailing. Below, we compare results obtained with $\epsilon = 0.2$, $\epsilon = 0$ (no net biosphere growth), and in some cases with $\epsilon = -0.2$. Attempts are being made to learn more about the role of the biosphere by determining the change in the atmospheric $^{13}C/^{12}C$ ratio since the beginning of industrialization, because the value of this ratio in organic carbon is very different from the values in atmospheric and oceanic CO_2 (*27*). Besides measurements in tree ring series, continuous $^{13}C/^{12}C$ measurements of atmospheric CO_2 or perhaps of CO_2 enclosed in old polar ice might be helpful for this purpose.

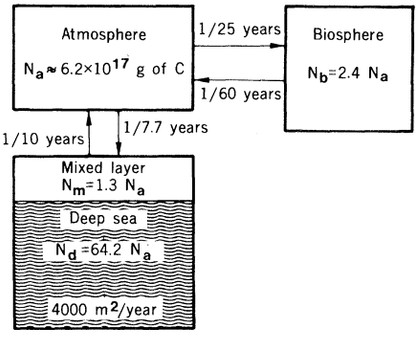

Fig. 1. Global CO_2 model with an eddy-diffusive deep-sea reservoir. The numerical values given are for the reservoir sizes, the exchange coefficients, and, in the deep sea, the eddy diffusivity.

The marine biosphere is not considered because it is of negligible influence. The carbon mass of living matter in the sea is only about 1/600 of the atmospheric CO_2. Furthermore, an increased carbon supply cannot lead to increased productivity of the marine biomass because the productivity is limited by phosphorus (*28*), not by carbon, which is abundant anyhow. [In some coastal zones the marine biota are being fertilized by excess phosphorus from human activities (*29*), but for a global budget this is of minor importance.]

The model parameters used and the individual models compared are summarized in Table 1. The models were modified to test the sensitivity of the predictions to changes in the most important modeling features: ocean mixing, buffer factor, and biosphere response. The thickness of the mixed layer and the exchange parameters (k_{am} and K for the BD models and k_{am} and k_{dm} for the 2B model) are chosen as described above.

Table 1. General model parameters and specific models used. "Theoretical ξ" means a buffer factor as given by Eq. 1. In model 4, a lower buffer factor is assumed. Models 1 and 4 include enhanced biosphere growth at higher CO_2 levels ($\epsilon = 0.2$), model 3 a net shrinking of the biosphere and models 2 and 5 a constant biospheric mass.

	Parameters common to all models	
N_a	Preindustrial CO_2 in atmosphere	~292 ppm = 6.2×10^{17} g of carbon; see below
N_b	Preindustrial CO_2 in biosphere	$2.4\,N_a$
N_{oc}	Preindustrial CO_2 in ocean	$65.5\,N_a$
N_m	Preindustrial CO_2 in mixed layer	$1.3\,N_a$ (BD); $5.3\,N_a$ (2B)
k_{am}	Exchange coefficient, atmosphere-mixed layer	1/7.7 years
k_{ab}	Exchange coefficient, atmosphere-biosphere	1/25 years
K	Eddy diffusion coefficient, deep sea, for BD	4000 m²/year
k_{dm}	Exchange coefficient, deep sea-mixed layer, for 2B	1/1250 years
ξ	Buffer factor for excess CO_2	See below
ϵ	Biosphere growth factor	See below
	Specific models and parameters	
Box diffusion (BD)		
1)	BD with theoretical ξ, $\epsilon = 0.2$, $N_a = 295$ ppm (6.25×10^{17} g of carbon)	
2)	BD with theoretical ξ, $\epsilon = 0$, $N_a = 291.5$ ppm (6.18×10^{17} g of carbon)	
3)	BD with theoretical ξ, $\epsilon = -0.2$, $N_a = 287.5$ ppm (6.10×10^{17} g of carbon)	
4)	BD with $\xi = 7$, $\epsilon = 0.2$, $N_a = 297.5$ ppm (6.31×10^{17} g of carbon)	
Two-box ocean (2B)		
5)	2B with theoretical ξ, $\epsilon = 0$, $N_a = 291.5$ ppm (6.18×10^{17} g of carbon)	

Validity of the Models

Keeling and co-workers (*30*) have continuously monitored the atmospheric CO_2 level at Mauna Loa, Hawaii, and at the South Pole. In Fig. 2 the observed CO_2 concentrations are compared with the predictions of models 1 to 3 of Table 1, based on the actual CO_2 production rates (*31*).

The preindustrial atmospheric CO_2 level, N_a, is not exactly known; it is probably somewhere between 288 and 295 parts per million (ppm), but even values outside this range cannot be ruled out (*32*). We assumed N_a for each model so that the predicted CO_2 concentration for 1971 was within $\pm$ 0.2 ppm of the observed mean value of 326.5 ppm. The values for N_a thus determined (Table 1) are compatible with the observed values (*32*). We wish to point out that in the BD models, N_a is the only parameter adjusted to measured CO_2 data; all other parameters are fixed independently. In the 2B model, the mixed-layer depth is also determined from CO_2 observations. Therefore, the 2B results up to 1975

agree closely with the BD curves with corresponding biota growth and buffer factors and are not shown in Fig. 2.

Comparing the world CO_2 production and CO_2 increase between 1958 and 1974, we find that the atmospheric increase was on the average 53 percent of the production. Assuming for a moment that this figure also applies for the cumulative production of 62 ppm until 1974, the original atmospheric level, N_a, is found to be about 296 ppm. The observed concentration curve shows changes in the rate of increase that are not predicted by the models and cannot be attributed to varying CO_2 production. Obviously the exchange parameters between the CO_2 reservoirs are not quite constant with time. We must be aware that relatively small fluctuations in environmental parameters are sufficient to produce CO_2 variations of the observed size, because the total fluxes are much larger than the net fluxes. Thus, the exchange flux between the atmosphere and the ocean is 330 ppm per 7.7 years or 43 ppm/year, while the net flux into the ocean is about 1 ppm/year—that is, about 2 percent of the total flux. Because of the slightly irregular CO_2 increase, the comparison of model computations with observations is not a very decisive model test. However, the BD case with a net decrease of the biosphere ($\epsilon = -0.2$, lowermost curve in Fig. 2) must be ruled out, whereas the case with $\epsilon = 0$ still appears possible. The best fits are achieved with $\epsilon = 0.2$, with either assumption for ξ.

The role of the biosphere needs further discussion, because the biomass may be decreasing because of human use. Woodwell and Houghton (*25*) even supposed that the net biospheric CO_2 flux into the atmosphere might be as high as the fossil flux. The atmospheric CO_2 variations depend, of course, on the time function of CO_2 production; let us assume that the nonfossil flux was always equal to the fossil flux—that is, increased about exponentially with a time constant of ~35 years. For this case, it can easily be seen that such a large total CO_2 production is not compatible with the current ideas about the CO_2 cycle, because the ocean would then have to be a much more effective sink than is suggested by the model calculations. The cumulative production up to 1974 would be twice the fossil production, or 124 ppm, of which about 38 ppm (= 330 ppm − 292 ppm) would reside in the atmosphere, with the rest in the ocean. For a buffer factor of 10 and a 38-ppm atmospheric excess, the ocean could take up, after infinite time

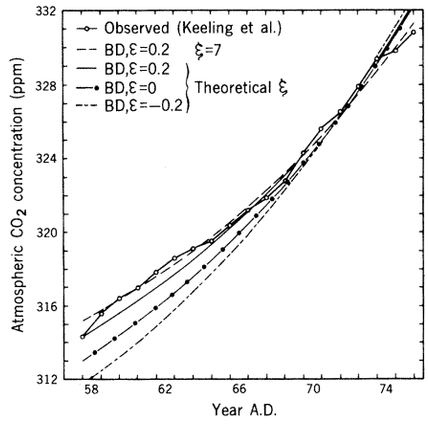

Fig. 2. Observed CO_2 concentrations as measured by Keeling and co-workers, average of South Pole and Mauna Loa data (*30*), and curves computed by use of models 1 to 4 of Table 1. Theoretical ξ means a buffer factor of about 9 and increase with higher CO_2 concentration (see Eq. 1).

(that is, at chemical equilibrium with the atmosphere), about 250 ppm of excess CO_2 (see Eq. 2). This means that if the biosphere had actually released as much CO_2 as stemmed from fossil carbon, the ocean would have reached 34 percent saturation by absorbing 86 ppm of CO_2. This corresponds to an effective depth of saturation of 1300 m, while in case of a constant biomass the ocean is only 10 percent saturated, corresponding to an effective depth of 380 m. A penetration depth of 1300 m for an *e*-folding time of about 35 years is in clear disagreement with the oceanic turnover time of at least 1000 years. Therefore, the high biospheric flux proposed by Woodwell and Houghton cannot be accounted for by faster oceanic mixing than we have assumed. On the other hand, Bolin (*26*), evaluating data of the Food and Agriculture Organization on world forest resources, estimated the present annual nonfossil carbon input to be 10 to 35 percent of the present emission from the use of fossil fuels. Our BD computations for $\epsilon = -0.2$ yield only 10 percent for this ratio, and for 35 percent the biota growth factor ϵ would have to be correspondingly more negative. As we have ruled out even the case $\epsilon = -0.2$ on the basis of Fig. 2, we see that Bolin's estimate, too, contradicts our model results.

The oceans could, however, take up more excess CO_2 than has been computed if the seawater buffer factor were lower than 9 to 10. But the thermodynamic constants entering into the calculations of the buffer factor are well determined and the average seawater composition is also reasonably well known, so it seems doubtful that the theoretical value is much in error. Another mechanism that might remove excess CO_2 is dissolution of near-surface carbonate sediments due to acidification of the seawater by the higher CO_2 concentration (see below), which would correspond to a lower apparent buffer factor. But this process is probably unimportant on a global scale. We therefore cannot find a sink for the proposed large CO_2 release from the biosphere.

The foregoing discussion is based, however, on the assumption that both fossil and biogenic CO_2 production rates grew in an approximately exponential way. This may be wrong for deforestation, in which case the situation is more complex. Actually, data for New England (*25*) show that the forest biomass in that region decreased greatly during the last century and has somewhat recovered since 1900. Of course, a large CO_2 input in the past does not contribute to an atmospheric increase today, but rather leads to a slightly declining "baseline." This shows that more data about variations of the terrestrial biomass are urgently needed; also, the oceanic buffering mechanism should be checked again.

On the basis of the discussion above, we prefer the following model characteristics: a diffusive deep sea (BD); a biosphere growth factor of $\epsilon = 0.2$ or 0; and a buffer factor ξ, judging purely from Fig. 2, of 9 to 10 (theoretical value) or somewhat lower. Thus, there remain cases 1, 2, and 4 from Table 1; cases 3 and 5 are not considered good approximations. Nevertheless, results for the 2B model (*5*) are presented below for comparison.

Model Responses

After a long time, any CO_2 input into the system will be distributed among the different reservoirs, the carbon contents of which will then be at new steady-state values. The total input is $n_a + n_{oc} + n_b$, where the n_i denote the excesses over the preindustrial CO_2 masses, N_i, in the atmosphere, ocean, and biosphere. At steady state, according to the definitions of ξ and ϵ, this is equal to

$$n_a + (1/\xi)(n_a/N_a)N_{oc} + \epsilon(n_a/N_a)N_b = (n_a/N_a)(N_a + N_{oc}/\xi + \epsilon N_b)$$

Therefore, the fraction F_a of the total input remaining in the atmosphere forever, according to the model, is given by

$$F_a = \frac{N_a}{N_a + N_{oc}/\xi + \epsilon N_b} \qquad (2)$$

Table 2. Cumulative CO_2 production, P_{cum}, and airborne fraction of P_{cum}, F_a (see Eq. 2). The models are described in Table 1.

Year	P_{cum} (ppm)	F_a (percent)			
		Model 1	Model 2	Model 4	Model 5
1970	53.9	56.3	62.2	51.4	62.4
		*Lower limit**			
2020	173	51.1	58.4	44.2	61.1
2070	293	45.7	54.1	37.7	59.2
2170	532	40.8	49.6	31.1	56.0
		Upper limit†			
2020	438	64.6	71.1	55.5	70.4
2070	2150	69.2	80.4	48.2	82.6
2170	3340	53.6	74.6	27.2	79.8

*Based on a constant production rate after 1975. †Assuming that P_{cum} increases as a logistic function of time after 1970 to 11.5 N_a.

Table 3. Estimates of P_{cum} and F_a for a maximum atmospheric CO_2 level of 438 ppm.

Year	Atmospheric CO_2 (ppm)	Model 1		Model 2		Model 4		Model 5	
		P_{cum} (ppm)	F_a (%)	P_{cum} (ppm)	F_a (%)	P_{cum} (ppm)	F_a (%)	P_{cum} (ppm)	F_a (%)
2020	395	190	52.7	175	59.0	209	46.6	169	61.0
2070	431	304	44.6	268	51.9	357	37.4	245	56.7
2170	438	406	35.2	350	41.8	506	27.8	309	47.3

For $\xi = 10$, we get $F_a = 0.125$ for $\epsilon = 0.2$ and 0.132 for $\epsilon = 0$. With higher concentrations, the buffer factor, and therefore also F_a, increases. The exploitable fossil fuel reserves have been estimated as 7.1×10^{12} metric tons of carbon (*9*) or about 11.5 times the preindustrial atmospheric amount of CO_2. If all these reserves were burned, the new steady-state concentration, for $\epsilon = 0$, would be about four times the preindustrial value (with $\xi = 23$ according to Eq. 1), accompanied by a temperature increase of 3° to 6°K (*3*). This state would be reached only after many centuries; before then, much higher CO_2 levels would occur.

The dynamic behavior of a linear model is fully characterized by its response to a pulse input. The solution of any input function can be represented as a superposition of such pulse responses. Our models are linear as long as ξ is constant, which is the case for relatively small CO_2 increases. Nevertheless, the linear pulse responses give a good idea about the general model behavior for larger concentrations too. Figure 3a shows the pulse responses for BD with $\epsilon = 0.2$ and $\epsilon = 0$ and for 2B with $\epsilon = 0$. Obviously, there are considerable differences between the different cases. The mixed layer rapidly reaches chemical equilibrium with the atmosphere, with a time constant (for a 75-m-deep mixed layer) of about 1.5 years (*21*). This is reflected in the quick decrease of the atmospheric CO_2 level during the first years after the pulse input. The mixed layer of the 2B ocean is about four times larger than that of the BD ocean and can take up correspondingly more excess CO_2; therefore, the decline at the beginning is stronger for the 2B than for the BD curves. However, when the CO_2 pressures of the mixed layer and the atmosphere have become approximately equal, CO_2 is transported faster into the eddy-diffusive than into the well-mixed deep sea. There is quite a large difference between the runs with and without biosphere growth ($\epsilon = 0.2$ and 0, respectively), demonstrating the importance of the terrestrial biosphere for the CO_2 cycle.

The CO_2 decrease is far from exponential (see Fig. 3b), and one can therefore not speak of one relaxation time or time constant for this decline. Thus, in BD with $\epsilon = 0.2$, it takes 21 years until the transient excess (that fraction of the excess above the final equilibrium value), which is plotted in Fig. 3b, has reached half its original value. One-quarter of the original value is only reached after 70 more years, and we have to wait another 240 years, or about 330 years in all, until the value has halved again to one-eighth. After the first decade, the concentration decreases most rapidly for BD with $\epsilon = 0.2$.

Predictions

A detailed prediction of future burning rates of fossil fuel would have to be speculative, but we can indicate upper and lower limits for this function with some confidence. As a lower limit we assume a constant CO_2 production rate at the level of 1975—that is, 1.87×10^{16} g of CO_2, equivalent to 2.4 ppm/year (*31*). Figure 4

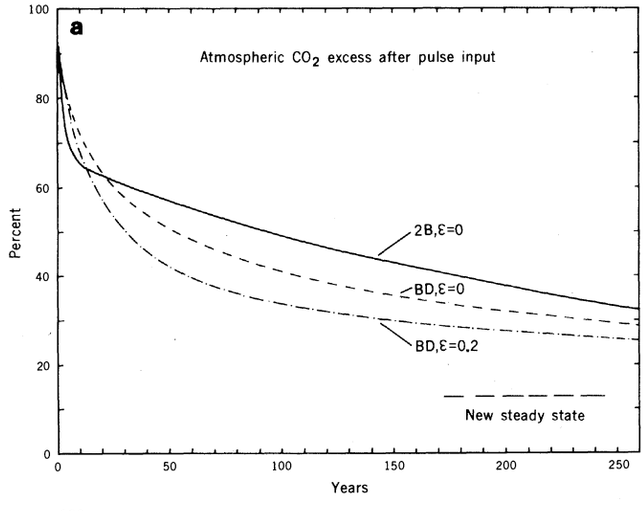

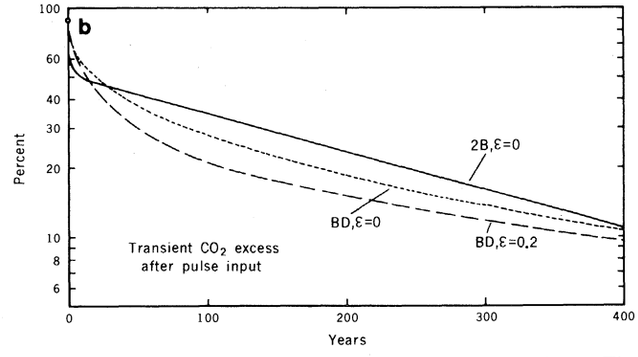

Fig. 3. (a) Responses of models 1, 2, and 5 to a CO_2 pulse input. The models are as described in Table 1, except for a constant buffer factor $\xi = 10$ (linear scale). (b) Same as (a), but only the transient part of the airborne fraction—that is, the part of the atmospheric CO_2 excess that will have vanished into the ocean or the biosphere after infinite time (logarithmic scale).

shows the results for this case. (Only the predictions for BD, with the theoretical ξ and $\epsilon = 0$ as well as $\epsilon = 0.2$, are shown in Figs. 4 to 6; Tables 2 and 3 show results for cases 4 and 5 as well.) It is noticed that no new equilibrium concentration is reached for a constant production rate, although this would be expected, for instance, for man-made aerosols, for which, because of their short atmospheric residence time, the rate of removal would soon equal the production rate. The fraction of the cumulative CO_2 production residing in the atmosphere is between 51 and 62 percent in 1970, and in 2070, 100 years later, is still between 38 and 59 percent (see Table 2). A doubled CO_2 level would be reached between the years 2160 and 2480.

As an upper limit we assume that all economically exploitable fossil fuels (11.5 times the preindustrial atmospheric CO_2; see above) will be burned, and that the production rate grows by 5.0 percent per year immediately after 1970, as it did from 1960 to 1970. The cumulative production is assumed to increase as a logistic function of time after 1970, so the production rate is given by

$$p(t) = \frac{d}{dt} \frac{3340 \text{ ppm}}{1 + 84 \exp(-t/20 \text{ years})}$$

Figure 5 shows $p(t)$ and the predictions. The CO_2 concentration would have doubled by the year 2020, essentially independent of the model used. The maximum atmospheric CO_2 level, five to ten times the preindustrial value, would be reached 40 to 80 years after the production peak, which is assumed to occur around 2060.

For the upper-limit scenario, the airborne amount of the cumulative production would be between 48 and 83 percent in 2070 (Table 2). For any future CO_2 production function between the two limiting cases discussed, 46 to 80 percent of the total produced CO_2 would still be in the atmosphere 100 years from now, according to the preferred models (cases 1 and 2). Thus, the assumption that the airborne fraction will remain near 50 percent, which is sometimes made (*4, 7*), may lead to a considerable underestimation of future CO_2 levels. It is mainly the dependence of the oceanic buffer mechanism on the CO_2 concentration that is responsible for the high atmospheric load, because at high concentrations the ocean becomes quite ineffective as a CO_2 sink.

Comparing the various predictions, we see that the concentrations obtained with the BD model are lower than those obtained with the 2B model (Table 2). This

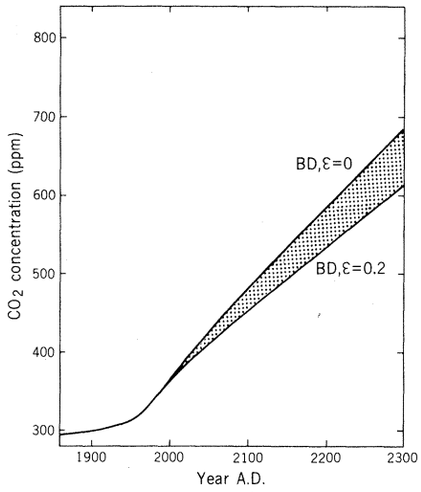

Fig. 4. Predictions of future atmospheric CO_2, assuming a constant production rate of 2.4 ppm/year after 1970. Only the results for a diffusive deep sea and for the theoretical buffer factor ξ (see Eq. 1) are given, for a constant ($\epsilon = 0$) and a growing ($\epsilon = 0.2$) biosphere. The shaded area indicates the concentration range which we consider the most realistic.

is because diffusive transport into the deep sea is faster, for short-time disturbances, than transport by exchange between two boxes, as discussed in (*19*). The difference between the BD cases with $\epsilon = 0.2$ and $\epsilon = 0$ (models 1 and 2) demonstrates the importance of any variation of the terrestrial biomass. The assumption of a positive biota growth factor ϵ, constant over centuries, is probably not justifiable. Thus, case 1 predicts in the upper limit 100 percent growth of the biosphere by the year 2200.

With climate models becoming more and more realistic, a maximum permissible atmospheric CO_2 level might be found which should not be exceeded if the atmospheric radiation balance is not to be disturbed in a dangerous way. We do not know such a threshold level at present; let us assume that it would be 50 percent above the preindustrial concentration. This would lead, according to present climate models, to a mean temperature increase of about 1° to 2°K (*3*). The question is, What amounts of fossil fuels may be burned in the future in order not to exceed this 50 percent excess? We have computed these production time histories (*33*) under the assumption that the constant 50 percent excess is reached asymptotically as a logistic function of time (see Fig. 6). The fastest increase of the CO_2 level occurs in the year 2000, and computed CO_2 emission rates are largest between 2000 and 2010—28 to 84 percent above the 1970 value, depending on the model considered. Then they have to level off rapidly, reaching 1970 values between 2030 and 2080. In 150 to 250 years from now, the decrease becomes very slow and the permitted output remains for a long time at 25 to 40 percent of the 1970 rate. The yearly consumption at the end of our century would, of course, be much smaller—by a factor of 2 to 3—than that in our upper-limit case. The integral production would, 100 years from now, be of the order of one preindustrial atmospheric CO_2 mass (Table 3).

This scenario clearly does not allow us to go on burning fossil fuel at the present growth rate for a long time. A modestly

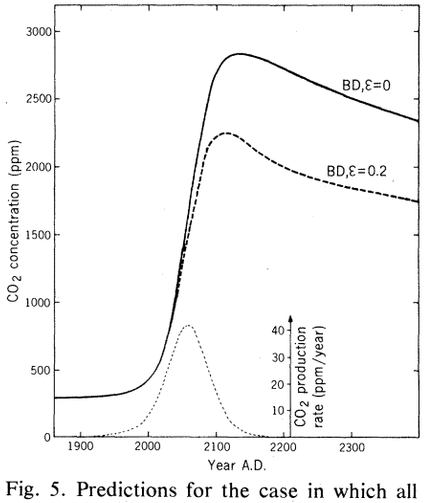

Fig. 5. Predictions for the case in which all recoverable fossil fuel is burned. The lowermost curve shows the assumed CO_2 production rate. The concentration curve for $\epsilon = 0.2$ is dashed because it would predict extensive growth of the biota, which does not seem very probable.

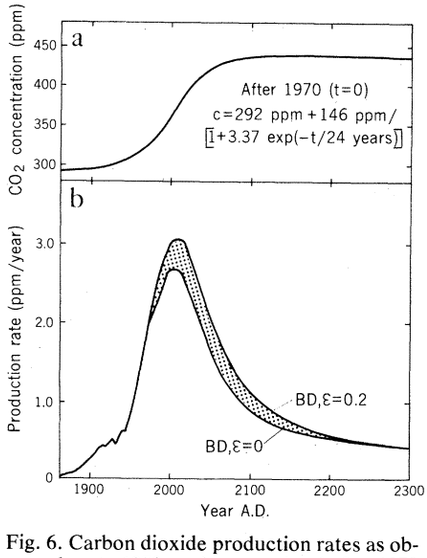

Fig. 6. Carbon dioxide production rates as observed up to 1970, and as permitted after 1970 for an increase of the atmospheric excess in a prescribed way (a) to a maximum of 50 percent.

growing demand for fossil energy could be met, but around the turn of the century new technologies would have to take over a substantial part of global energy production. Whatever model case is considered, the CO_2 output in the year 2000 permitted by this scenario is much lower than the value of 6 ppm/year recommended for modeling by Rotty (*34*).

It must be emphasized that we have arbitrarily chosen the limit of 50 percent for the allowable CO_2 excess, and it may be too low or too high. It merely serves to illustrate the concept of an energy strategy based on a maximum permissible atmospheric CO_2 increase.

Further Consequences

It has been mentioned that with an increasing CO_2 level the ocean might become undersaturated in CO_3^{2-}, so that the carbonate compensation level might rise and carbonate sediments be dissolved at depth. Once the dissolution of sedimentary carbonate started, the ocean's capacity for taking up industrial CO_2 would increase (*5, 35*). Eventually, even the surface ocean might become undersaturated in CO_3^{2-}, which would threaten the existence of organisms that build calcareous shells; however, surface waters are generally very supersaturated in CO_3^{2-} (*28*), so this danger does not exist in the near future, except perhaps in a few limited areas. We do not want to discuss these problems because (i) the kinetics of carbonate dissolution are not yet fully understood, and (ii) for a study of the oceanic carbonate system, the oceanic circulation and fluxes have to be considered in more detail than they are in global models designed for computing atmospheric CO_2 levels. For instance, the Atlantic and Pacific oceans should be separated because their turnover times and carbonate concentration patterns are significantly different. The formation of deep water at high latitudes by sinking of dense surface water should be considered.

Several authors (*35, 36*) have suggested that higher CO_2 concentrations would lead to enhanced continental weathering of minerals, and thus to a higher calcium input into the oceans, tacitly assuming that the weathering capacity of terrestrial waters is determined by the atmospheric CO_2 partial pressure. However, this is not the case in general, since the equilibrium CO_2 pressure in soil waters and in rivers is usually much higher than the atmospheric level, on the average by about one order of magnitude in the rivers of the world (*37*). This is so because most CO_2 is taken up by the infiltrating water in the top soil zones, where biogenic CO_2 is present at high concentrations. An increase in dissolved CO_2 and, therefore, weathering capacity could thus be caused only indirectly—for instance, through enhanced biospheric activity or a more intensive hydrologic cycle—and would be relatively small compared to the atmospheric CO_2 increase.

There are several feedback mechanisms that have not been mentioned so far. An amplification of the greenhouse effect leads to a warmer ocean surface and thus a lower CO_2 solubility, so that the atmospheric CO_2 pressure grows even more. Eriksson (*38*) computed a 5 percent change of the CO_2 pressure per degree centigrade for equilibrium between atmosphere and ocean. If a doubling of the CO_2 concentration (to ~580 ppm) leads to a warming of 1.5° to 3°K, this would bring about another CO_2 increase of approximately 7.5 to 15 percent, or 44 to 87 ppm. This first-order estimate shows that this feedback effect is quite appreciable. As pointed out by Eriksson, however, it would take a very long time for the whole ocean to reach equilibrium, so that the effect would be smaller on the time scales considered here.

According to Manabe and Wetherald (*2*), not only temperature but also amount of precipitation would rise with a higher CO_2 level. Both changes are favorable for biological productivity (*39*), so that growth of the biosphere is suggested not only on the basis of its dependence on CO_2. Whether these favorable tendencies would prevail over the negative influences on vegetation—extensive human use and air pollution—can only be decided when adequate data are obtained.

Finally, one should keep in mind the question of what factors determine the natural atmospheric CO_2 pressure in the long term, which has not yet been clearly resolved (*15*). Geologic processes that are not discussed here then become important, and the problem is even more complicated than when one considers only variations over centuries.

Conclusions

It has often been noted that about 50 percent of the total CO_2 produced remains in the atmosphere. Bacastow and Keeling (*10*) found, however, that the buffer factor of seawater increases with higher atmospheric CO_2 concentration, which means that the ocean becomes a less effective sink for industrial CO_2. For our upper-limit scenario (all fossil reserves to be burned) the airborne fraction may be as high as 80 percent. After CO_2 production stopped, the atmospheric level would decline very slowly to a new equilibrium state. At equilibrium, the atmosphere would still contain at least one-eighth of the total man-made CO_2. This clearly shows that, once negative effects of the CO_2 increase were observed, it would not be possible to restore the "pre-CO_2" situation simply by stopping CO_2 emissions.

If a maximum CO_2 increase of 50 percent above the preindustrial concentration is tolerable, CO_2 production could still be increased until the beginning of the 21st century, but it would then have to be reduced rapidly. The value of 50 percent for the tolerable increase may be too high or too low; if it is correct, we may burn in total over the next centuries not much more than 10 percent of the known fossil fuel reserves.

Our intention in this article is to present the results that can be obtained by means of relatively simple global models and to indicate the uncertainties still involved. The following are some major problems that are still open.

1) *Biospheric masses and fluxes*. The biomass has probably decreased in some places and increased in others. Is the observed CO_2 increase partly due to a shrinking biosphere, or did the biosphere as a whole take up fossil CO_2?

2) *The oceanic buffer mechanism against CO_2 variations*. There is a discrepancy between thermodynamic computations (*6, 10*), which yield a buffer factor ξ of 9 to 10, and experimental results (*22*), which yield $\xi \approx 7$. Unfortunately, it is difficult to measure the increase of the total CO_2 concentration in the sea, which presently amounts to only about 1 percent in surface waters, while natural variations (for example, with latitude) are much larger.

References and Notes

1. R. M. Goody and J. C. G. Walker, *Atmospheres* (Prentice-Hall, Englewood Cliffs, N.J., 1972).
2. S. Manabe and R. T. Wetherald, *J. Atmos. Sci.* **32**, 3 (1975).
3. S. Schneider, *ibid.*, p. 2060.
4. C. F. Baes, H. E. Goeller, J. S. Olson, R. M. Rotty, *The Global Carbon Dioxide Problem* (ORNL-5194, Oak Ridge National Laboratory, Oak Ridge, Tenn., 1976).
5. S. Bolin and E. Eriksson, in *The Atmosphere and the Sea in Motion*, B. Bolin, Ed. (Rockefeller Institute Press, New York, 1959), pp. 130–142.
6. W. S. Broecker, Y.-H. Li, T.-H. Peng, in *Impingement of Man on the Oceans*, D. W. Hood, Ed. (Wiley-Interscience, New York, 1971), pp. 287–324.
7. W. S. Broecker, *Science* **189**, 460 (1975).

8. L. Machta, in *The Changing Chemistry of the Oceans*, D. Dyrssen and D. Jagner, Eds. (Almqvist & Wiksell, Stockholm, 1972), pp. 121–145.
9. K. E. Zimen and F. K. Altenhein, *Z. Naturforsch. Teil A* **28**, 1747 (1973).
10. R. Bacastow and C. D. Keeling, in (*11*), pp. 86–135.
11. G. M. Woodwell and E. V. Pecan, Eds., *Carbon and the Biosphere* (Atomic Energy Commission, Technical Information Service, Washington, D.C., 1973).
12. C. D. Keeling, in *Energy and Climate: Outer Limits to Growth* (National Academy of Sciences, Washington, D.C., in press).
13. Data and models on the global carbon cycle have been summarized by Baes *et al.* (*4*), and by Bolin (*14*).
14. B. Bolin, *Sci. Am.* **223**, 131 (September 1970); in *The Physical Basis of Climate and Climate Modelling* (GARP Publ. Ser. No. 16, World Meteorological Organization, Geneva, 1975), pp. 225–235.
15. R. M. Garrels and E. A. Perry, in *The Sea*, E. G. Goldberg, Ed. (Wiley, New York, 1974), vol. 5, pp. 303–306.
16. For a summary of work on ^{14}C in the oceans see M. Stuiver, in (*11*), pp. 6–20.
17. C. D. Keeling, in *Chemistry of the Lower Atmosphere*, S. I. Rasool, Ed. (Plenum, New York, 1973), pp. 251–329.
18. K. Wyrtki, *Deep-Sea Res.* **9**, 11 (1962); W. H. Munk, *ibid.* **13**, 707 (1966); J. Craig, *J. Geophys. Res.* **74**, 5491 (1969).
19. H. Oeschger, U. Siegenthaler, U. Schotterer, A. Gugelmann, *Tellus* **27**, 168 (1975).
20. The natural ^{14}C variations, as observed in tree rings, seem to be larger than the ^{14}C variations calculated from models, including the BD model, under the assumption that they are due to varying ^{14}C production due to changing solar activity as reflected in sunspot numbers. However, this is not necessarily due to wrong model results for the attenuation factors, because the relationship between sunspot numbers and changes in ^{14}C production is not firmly established. Furthermore, there may be other reasons for ^{14}C variations, such as fluctuations in ocean mixing.
21. W. S. Broecker and T.-H. Peng, *Tellus* **26**, 21 (1974).
22. A. Rebello and K. Wagener, paper presented at the 4th International Symposium on the Chemistry of the Mediterranean, Rovinj, Yugoslavia, 1976.
23. W. A. Reiners, in (*11*), p. 303. The high carbon content of the terrestrial biosphere is obtained from an estimate of total nitrogen in organic detritus and a C/N ratio of 12.
24. H. Lieth, *J. Geophys. Res.* **68**, 3887 (1963).
25. G. W. Woodwell and R. A. Houghton, in *Dahlem Workshop on Global Chemical Cycles and Their Alternation by Man*, W. Stumm, Ed. (Abakon, Berlin, 1977), pp. 61–72.
26. B. Bolin, *Science* **196**, 613 (1977).
27. H. D. Freyer and L. Wiesberg, in *Isotope Ratios as Pollutant Source and Behaviour Indicators* (International Atomic Energy Agency, Vienna, 1975), p. 49; M. Stuiver, personal communication.
28. W. S. Broecker, *Chemical Oceanography* (Harcourt Brace Jovanovich, New York, 1974).
29. W. Stumm, in *The Changing Chemistry of the Ocean*, D. Dyrssen and D. Jagner, Eds. (Almqvist & Wiksell, Stockholm, 1972), pp. 329–346.
30. C. D. Keeling, R. B. Bacastow, A. E. Bainbridge, C. A. Ekdahl, P. R. Guenther, L. S. Waterman, J. F. S. Chin, *Tellus* **28**, 538 (1976); C. D. Keeling, J. A. Adams, C. A. Ekdahl, P. R. Guenther, *ibid.*, p. 552; C. D. Keeling, private communication. Note that the corrected scale ("1974 manometric mole fraction scale") used in these publications and also in this article is slightly different from the scale used formerly by Keeling and co-workers. The value for the end of 1971 is 326.5 ppm (new scale) compared to 322.5 ppm (old scale).
31. Data up to 1970 are from C. D. Keeling [*Tellus* **25**, 174 (1973)]; data for 1971 to 1974 are from R. M. Rotty (*34*); and the 1975 value (2.40 ppm/year) was estimated by Keeling (*12*).
32. G. S. Callendar, *Tellus* **10**, 243 (1958); J. R. Bray, *ibid.* **11**, 220 (1959).
33. The production functions leading to the prescribed CO_2 excess were computed by leaving the production rate constant for 1 year, then comparing the actual atmospheric concentration with the concentration aimed at (given in Fig. 6), correcting the production rate accordingly, continuing the procedure for one more year, and so on.
34. R. M. Rotty, *Global Carbon Dioxide Production from Fossil Fuel and Cement, A.D. 1950–A.D. 2000* (Institute for Energy Analysis Research Memorandum [IEA(M)-76-4], Oak Ridge Associated Universities, Oak Ridge, Tenn., 1976).
35. W. S. Broecker, in (*11*), pp. 32–50.
36. P. Möller and P. P. Parekh, *Sci. Total Environ.* **4**, 177 (1975).
37. R. M. Garrels and F. T. Mackenzie, *Evolution of Sedimentary Rocks* (Norton, New York, 1971), chaps. 5 and 6.
38. E. Eriksson, *J. Geophys. Res.* **68**, 3871 (1963).
39. R. H. Whittaker and G. E. Likens, in (*11*), pp. 281–302.
40. Thanks are due to M. Stuiver for stimulating discussions, and to W. S. Broecker and another reviewer, unknown to us, for valuable comments on this article. This work is financially supported by the Swiss National Science Foundation.

Origins of Prokaryotes, Eukaryotes, Mitochondria, and Chloroplasts

A perspective is derived from protein and nucleic acid sequence data.

Robert M. Schwartz and Margaret O. Dayhoff

Many proteins and nucleic acids are "living fossils" in the sense that their structures have been dynamically conserved by the evolutionary process over billions of years (*1*). Their amino acid and nucleotide sequences occur today as recognizably related forms in eukaryotes and prokaryotes, having evolved from common ancestral sequences by a great number of small changes (*2*). These sequences may still carry sufficient information for us to unravel the early evolution of extant biological species and their biochemical processes. There are two principal computer methods that can be used to treat sequence data in order to elucidate evolutionary history. These were first described more than 10 years ago (*3, 4*) and have been used to construct a vertebrate phylogeny from each of a number of proteins (*5–7*). This phylogeny is generally consistent with both the fossil record and morphological data. Only recently has enough sequence information become available from diverse types of bacteria and blue-green algae, and from the cytoplasm and organelles of eukaryotes, for us to attempt the construction of a biologically comprehensive evolutionary tree. These sequences include ferredoxins, 5*S* ribosomal RNA's, and c-type cytochromes. We describe here an evolutionary tree derived from sequence data that extends back close to the time of the earliest divergences of the present-day bacterial groups.

Knowledge of the evolutionary relationships between all species would have great predictive advantage in many areas of biology, because most systems within the organisms would show a high degree of correlation with the phylogeny. Knowing the relative order of the divergences of prokaryote types and their protein constituents is important to understanding the evolution of metabolic pathways. With such information the long-standing question of how eukaryote organelles originated might be resolved.

Before we consider the phylogenies based on sequence data, we will briefly review the fossil record and describe the time scale during which the various prokaryote groups diverged (*8, 9*). The early fossil record is sparse and subject to some uncertainty of interpretation. The oldest known bacterium-like structures that could possibly be biogenic are preserved in the Swaziland sediments and are more than 3.1 billion years old (*8,*

Dr. Schwartz is a senior research scientist at the National Biomedical Research Foundation. Dr. Dayhoff is an associate professor in the Department of Physiology and Biophysics at Georgetown University Medical School and Associate Director of Research at the National Biomedical Research Foundation at Georgetown University Medical Center, Washington, D.C. 20007.

0036-8075/78/0127-0395$02.00/0